Effect of exchange interaction in ferromagnetic superlattices: A Monte Carlo study

R Masrour† and A Jabar

Laboratory of Materials, Processes, Environment and Quality, Cady Ayyed University, National School of Applied Sciences, 63 46000, Safi, Morocco

(Received 6 January 2016; revised manuscript received 14 February 2016; published online 25 August 2016)

The Monte Carlo simulation is used to investigate the magnetic properties of ferromagnetic superlattices through the Ising model. The reduced critical temperatures of the ferromagnetic superlattices are studied each as a function of layer thickness for different values of exchange interaction. The exchange interaction in each layer within the interface and the crystal field in the unit cell are studied. The magnetic coercive fields and magnetization remnants are obtained for different values of exchange interaction, different values of temperature and crystal field with fixed values of physical parameters.

Keywords: Monte Carlo simulations, superlattice, critical temperature, magnetic coercive field

PACS: 75.40.Mg, 73.21.Cd, 68.35.Rh, 75.30.Cr− **DOI:** 10.1088/1674-1056/25/10/107502

1. Introduction

Magnetism in ultrathin film is now a fairly well established field of research, and has attracted much attention, both experimentally and theoretically.[1–4] The magnetic properties of hexagonal compact superlattices of materials A and B: a helimagnetic and a ferromagnetic phase, at low temperature, were studied in Ref. [5]. The ferromagnetic/antiferromagnetic superlattices, which are composed of a spin-1/2 ferromagnetic monolayer and a spin-1 antiferromagnetic monolayer with a single-ion anisotropy, respectively, have been investigated in Ref. [6]. The magnetization in (Fe 3 nm/Dy 2 nm) multilayers have been studied experimentally and numerically in Ref. [7]. The influences of the exchange coupling and single-ion anisotropy parameters in the model Hamiltonian on the martensitic–austenitic transformations were studied and analyzed in comparison with the results for hexagonal nanoparticles in Ref. [8]. To analyze the dependence of the critical temperature T_C on size, some authors[9–13] have considered the ferromagnetic nearest-neighbor Ising model of the simple cubic lattices for film of c layer. The magnetic coupling at the surface, J_S, may be identical with or different from that in the bulk, J_b. Transition temperature of a multilayer consisting of spin-1/2 and spin-3/2 ferromagnetic Ising layers has been computed by using the effective field theory[14–16] in order to explain the experimental data of rare earth/transition metal multilayer films, respectively. Mean-field theory has also been used to study magnetic properties of rare earth/transition multilayers,[17] but very few Monte Carlo studies dealt with the rare earth/transition metal multilayer systems. The phase transition and magnetic properties of a ferromagnet spin-S, a disordered diluted thin and semi-infinite film with a face-centered cubic lattice are investigated by using the high temperature series expansions technique extrapolated with Padé approximants method for Heisenberg, XY and Ising models in Ref. [18]. The magnetic properties of ferromagnetic Ni/Au core/shell have been studied by using Monte Carlo simulations within the Ising model in Ref. [19]. Hysteresis loops, micromagnetic structures, and hysteresis loop area curves, as well as dynamic correlation between the magnetization and the external field have been studied each as a function of the field and film parameters in Ref. [20]. Recently, we have used the Monte Carlo simulations to study the magnetic properties of a nanowire system based on a honeycomb lattice in the absence and presence of both an external magnetic field and crystal field.[21] The purpose of this work is to explore the variations of magnetization and magnetic susceptibility with the reduced temperature, exchange interaction between bilayers and zero crystal field for a fixed value of exchange interaction in surface and in bulk with different sizes. The critical temperatures are obtained for different values of size l_a and for different values of exchange interactions between bilayers. The magnetic hysteresis cycle with reduced crystal field, exchange interaction between bilayers and reduced critical temperatures are established. From these curves we deduce the coercive field and magnetization remnant.

2. Model and formulation

We consider superlattices of ferromagnetic materials a and b, with a simple cubic structure. The l_a and l_b are the corresponding numbers of atomic layers in materials a and b, respectively. $l = l_a + l_b$ is the thickness of the unit cell (see Fig. 1). In all text, $l_b = 7$ unless otherwise stated.

The Hamiltonian for the a and b ferromagnetic superlattices includes the interactions between the nearest neighbors,

†Corresponding author. E-mail: rachidmasrour@hotmail.com

© 2016 Chinese Physical Society and IOP Publishing Ltd

external magnetic field, and the crystal field is given as

$$H = -J_{aa}\sum_{\langle i,j\rangle}\sigma_i^a\sigma_j^a - J_{Sa}\sum_{\langle i,j\rangle}\sigma_i^{Sa}\sigma_j^{Sa} - J_{ab}\sum_{\langle i,j\rangle}\sigma_i^a S_j^b - J_{bb}\sum_{\langle i,j\rangle}S_i^b S_j^b - J_{Sb}\sum_{\langle i,j\rangle}S_i^{Sb}S_j^{Sb} - h\sum_i(\sigma_i^z + S_i^z) - \Delta\sum_i\left((\sigma_i^z)^2 + (S_i^z)^2\right), \quad (1)$$

where $\langle i,j\rangle$ refers to the first nearest neighbor sites i and j, Δ represents the crystal field, and h is the external magnetic field. The (J_{Sb} and J_{Sa}), J_{ab}, J_{aa}, and J_{bb}, are the exchange interactions parameters between the two nearest-neighbor magnetic particles at the surfaces of materials (a and b), the exchange coupling between nearest neighbour spins across the interface, in the bulk materials a and b , respectively (see Fig. 1). The spin moments of magnetic atoms in layers of materials a and b, are $\sigma_i^{Sa} = \sigma_i^a = 2$ and $S_i^{Sb} = S_i^b = 3/2$, respectively. In full text, the new parameters are $R_1 = J_{Sa}/J_{aa} = R_3 = J_{Sb}/J_{aa} = R_4 = J_{bb}/J_{aa} = 1$.

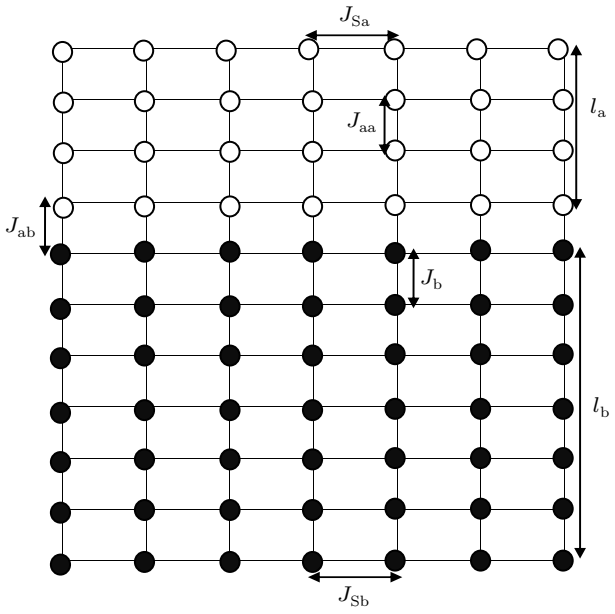


Fig. 1. Ferromagnetic materials a and b superlattices with the thickness of the cell being $l_a + l_b$.

3. Monte Carlo simulations

The ferromagnetic materials a and b superlattices are assumed to reside in the unit cells and the system consists of the total number of spins $N = (l_a + l_b)l$, with $l = 8$, $l_b = 7$ and $l_a = 5$, 7, 9, 11 where $(l_a + l_b)$ is the system size as given in Fig. 1. We use a standard sampling method to simulate the Hamiltonian given by Eq. (1). Cyclic boundary conditions on the lattice are imposed and the configurations are generated by sequentially traversing the lattices and making single-spin flip. The flips are accepted or rejected according to a heat-bath algorithm under the Metropolis approximation. Our data are generated with 10^5 Monte Carlo steps per spin, discarding the first 10^4 Monte Carlo simulations. Starting from different initial conditions, we perform the average of each parameter and estimate the Monte Carlo simulations, averaging over many initial conditions. Our program calculates the following parameters:

the magnetization of superlattices

$$m = \left\langle \frac{1}{N}\sum_i\left(\sigma_i^a + S_i^b\right)\right\rangle; \quad (2)$$

the internal energy E per site

$$E = \frac{1}{N}\langle H\rangle, \quad (3)$$

the magnetic susceptibility

$$\chi = \beta\left(\langle m^2\rangle - \langle m\rangle^2\right), \quad (4)$$

where $\beta = 1/(k_B T)$, T denotes the absolute temperature, and k_B is the Boltzmann's constant.

4. Results and discussion

The superlattices of ferromagnetic materials a and b are investigated by Monte Carlo simulation. The transition temperatures each as a function of surface exchange constant are studied. Figure 2 shows the variations of magnetization and magnetic susceptibility with reduced temperature T/J_{aa} for $R_2 = 0.2$, respectively, with $\Delta/J_{aa} = 0.0$, $R_1 = J_{Sa}/J_{aa} = R_3 = J_{Sb}/J_{aa} = R_4 = J_{bb}/J_{aa} = 1$ and $l_a = 5$, 7, 9, and 11. The temperature dependences of the susceptibility are calculated for different lattice sizes in order to estimate the reduced critical temperature, T_C/J_{aa}. The position of the susceptibility maximum is allowed to be used to estimate the range of values of the critical temperature. The critical temperatures are obtained for each layer from the divergence (or the situation of peak) of magnetic susceptibilities at the reduced critical temperature. The obtained values are all 9 for $l_a = 7$, 9, 11 with $R_2 = 0.2$ and $h/J_{aa} = 0.4$. This value is superior to those obtained by high temperature series expansions[22] and those obtained by effective field theory.[23,24]

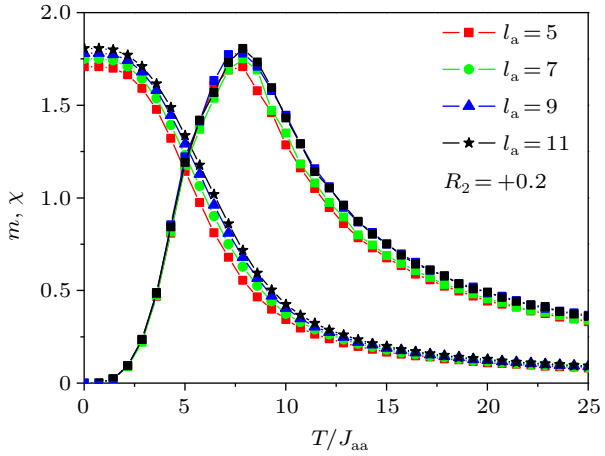


Fig. 2. (color online) Variations of magnetization and magnetic susceptibilities with reduced temperatures T/J_{aa} for $R_2 = 0.2$ with $\Delta/J_{aa} = 0.0$ and $h/J_{aa} = 0.4$.

Figure 3 shows the variations of magnetization and magnetic susceptibilities with reduced temperature T/J_{aa} for $R_2 = J_{ab}/J_{aa} = 0.2$, 1.5, 3, 5 with $\Delta/J_{aa} = 0.0$, $h/J_{aa} = 0.4$, and $R_1 = R_3 = R_4 = 1.0$. The critical temperature is not very sensible with exchange interaction increasing. This behavior is comparable to those given in Refs. [22] and [25]. This behavior is similar to those obtained in Ref. [26] by using the Monte Carlo simulation in the case of mixed spins (2-1) hexagonal Ising nanowire with core–shell structure.

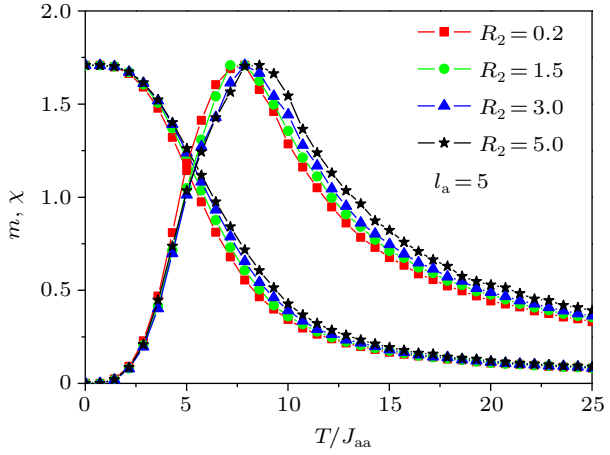


Fig. 3. (color online) Variations of magnetization and magnetic susceptibility with reduced temperature T/J_{aa} for $R_2 = 0.2$, 1.5, 3, 5 with $\Delta/J_{aa} = 0.0$ and $h/J_{aa} = 0.4$.

Figure 4 shows the variations of magnetization and magnetic susceptibilities with reduced temperature T/J_{aa} for different values of crystal field $\Delta/J_{aa} = 0$, -1, -1.5, -2 with $R_2 = 1$ with $R_1 = R_3 = R_4 = 1.0$. The critical temperature decreases with increasing the absolute value of a crystal field (see Table 1). A similar behavior is observed in the previous work[27] in which Monte Carlo simulation was conducted to investigate the phase diagrams of a ferrimagnetic cubic nanoparticle (nanocube) with a spin-3/2 core surrounded by a spin-1 shell layer with antiferromagnetic interface coupling. The variations of magnetization with reduced exchange interaction R_2 are given in Fig. 5. The plots of magnetization versus the R_2 with different reduced temperatures $T/J_{aa} = 1$, 1.5, 2, 2.5 with $L_a = 7$ are presented in Fig. 5(a). Presented in Fig. 5(b) are the plots of magnetization versus exchange interaction R_2 with $L_a = 5$, 7, 9, 11 for $T/J_{aa} = 1.5$. The magnetization increases with increasing R_2 and size of system and decreases with increasing reduced temperatures until it reaches saturation value. The same qualitative results have been obtained in early work.[28,29] The system may be ordered in the bulk earlier than at surfaces; and when the number of layers increases, the ordering temperature of the system tends to the bulk one. For $R_2 > 1.0$, the system may order in interface layers earlier than in the other layers, i.e., the interface magnetism dominates and when the number of layers is very large, the system can be considered practically as a two-constituents superlattice with a critical temperature depending on magnetic coupling at the interface R_2.

Table 1. Values of reduced critical temperatures for different values of crystal field Δ with $l_a = 5$ and $R_2 = 1$.

T_C/J_{aa}	7.85	6.23	5	3.52
Δ/J_{aa}	0	-1	-1.5	-2

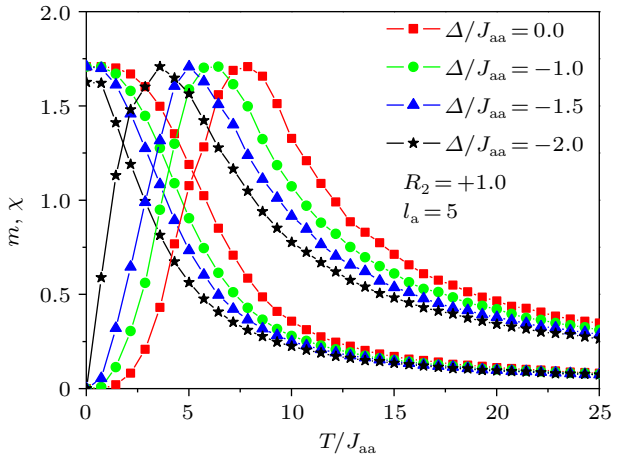


Fig. 4. (color online) Variations of magnetization and magnetic susceptibilities with reduced temperature T/J_{aa} for $\Delta/J_{aa} = 0.0$, -1.0, -1.5, -2.0, $R_2 = 1$, $h/J_{aa} = 0.4$, and $l_a = 5$.

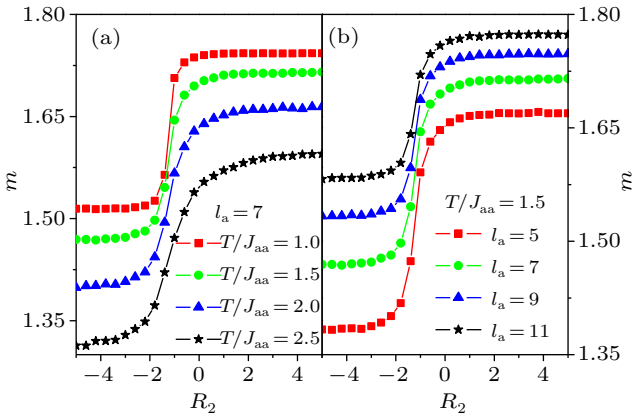


Fig. 5. (color online) Variations of magnetization with reduced exchange interaction R_2: (a) for $\Delta/J_{aa} = 1.0$, 1.5, 2.0, 2.5, $l_a = 7$ and (b) for $l_a = 5$, 7, 9, 11, $T/J_{aa} = 1.5$, and $h/J_{aa} = 0.4$.

The variations of magnetization with reduced crystal field Δ/J_{aa} for ($T/J_{aa} = 1$, 2, 2.5, 3, $R_2 = 1$ and $l_a = 5$), for ($R_2 = 1$, 2, 3, 5, $T/J_{aa} = 1$ and $l_a = 5$) and for ($l_a = 5$, 7, 9, 11, $T/J_{aa} = 1$ and $R_2 = 1$), are given in Figs. 6(a)–6(c), respectively with $R_1 = R_3 = R_4 = 1.0$ and $h/J_{aa} = 0.4$. The magnetization increases with increasing the crystal field and deceases with increasing the reduced temperatures; magnetization increases with increasing the exchange interaction R_2 as shown in Figs. 5(a) and 5(b). The magnetization increases with increasing the size of system for $\Delta/J_{aa} > -2.47$ and decreases with reducing the size of system for $\Delta/J_{aa} - 2.47$.

The magnetic hysteresis cycles with the reduced exchange interactions $R_2 = 0.4$, 3.0, for a zero reduced crystal field and $T/J_{aa} = 1$ are shown in Figs. 7(a) and 7(b), respectively. The coercive field and remnant magnetization decrease with increasing the reduced exchange interaction R_2 between the bi-layers for fixed value of reduced temperature and crystal field. This behavior is observed in previous work.[30–32]

The saturation magnetization and coercive field are obtained for given specific unit-cell sizes. Our results are also in good agreement not only with those obtained experimentally,[33–37] but also with those estimated by the ab initio calculations in Ref. [38]. The magnetic hysteresis cycles with reduced crystal field $\Delta/J_{aa} = 0$ and -1 for $R_2 = 1$ and $T/J_{aa} = 3$ are shown in Figs. 8(a) and 8(b), respectively. The coercive field and remnant magnetizations decrease with increasing the reduced crystal field in the bi-layers for fixed values of reduced temperature and reduced exchange interactions R_2. A similar compositional dependence of the coercivity was also observed in CoPt and CoO nanoparticles synthesized using the reverse micelle method.[30,39] The increase of the reduced exchange interactions R_2 has no significant effect on coercive field nor on the remnant magnetization. The coercive field and remnant magnetizations decrease with increasing the reduced temperature as noted in Ref. [7]. The obtained results are similar to those obtained in Ref. [40]. The loop magnetic hysteresis cycle is observed at $R_2 = 1$, $\Delta/J_{aa} = -3$ and $T/J_{aa} = 3$ with $l_a = 5$. Moreover, the increase of the temperature softens the jumps of the hysteresis curve (Figs. 7 and 8), which disappears for higher temperatures, as has been experimentally observed in the above-mentioned Ce system.[41] Although the general trends of the experimental results are well described by the present results (symmetric hysteresis loops and evanescence of the jumps with increasing temperature), at this stage it is difficult to carry out a direct comparison with the experimental results. Finally, we show in Figs. 9(a) and 9(b) the magnetic hysteresis cycles with $l_a = 5$ and $l_a = 11$, respectively for a zero reduced crystal field, $R_2 = 0.4$ and $T/J_{aa} = 1$. The magnetic coercive field h_C increases with increasing the size. The observed increase in h_C is similar to previously reported results showing that h_C increases with film thickness decreasing.[42,43]

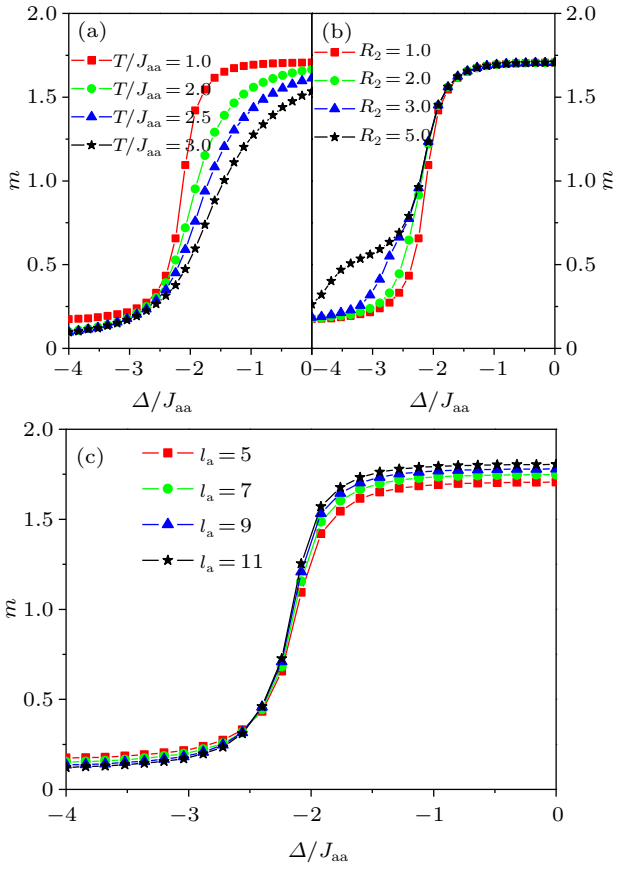


Fig. 6. (color online) Variations of magnetization with reduced crystal field Δ/J_{aa} (a) for $T/J_{aa} = 1.0$, 2.0, 2.5, 3.0, $R_2 = 1$ and $l_a = 5$, (b) for $R_2 = 1.0$, 2.0, 3.0, 5.0, $T/J_{aa} = 1$ and $l_a = 5$, and (c) for $l_a = 5$, 7, 9, 11, $T/J_{aa} = 1$ and $R_2 = 1$ with $h/J_{aa} = 0.4$.

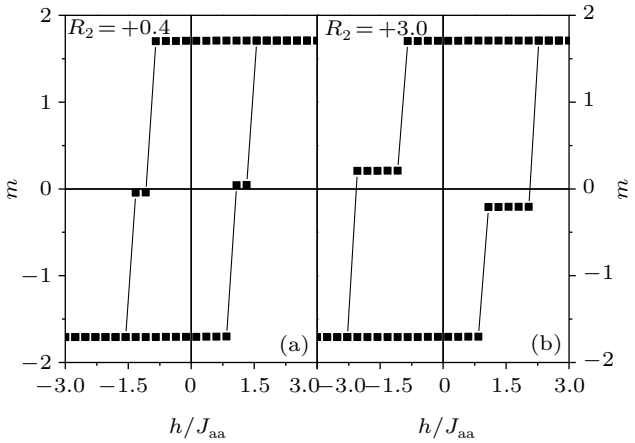


Fig. 7. Magnetic hysteresis cycles with the reduced exchange interaction $R_2 = 0.4$ (a), 3.0 (b) for a zero reduced crystal field, $T/J_{aa} = 1$ and $l_a = 5$.

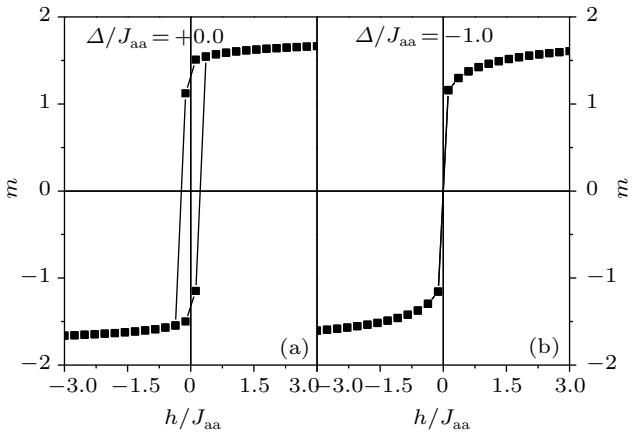


Fig. 8. Magnetic hysteresis cycles with the reduced crystal field $\Delta/J_{aa} = 0.0$ (a), -1.0 (b) for $R_2 = 0.4$, $T/J_{aa} = 3$, and $l_a = 5$.

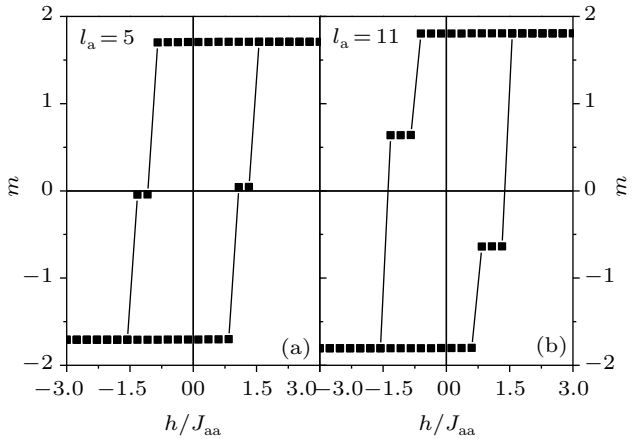


Fig. 9. Magnetic hysteresis cycles with $l_a = 5$ (a) and 11 (b) for a zero reduced crystal field, $R_2 = 0.4$ and $T/J_{aa} = 1$.

5. Conclusions

The Monte Carlo simulations are used to investigate the magnetic properties of the Ising model of infinite a and b ferromagnetic superlattices having simple cubic crystal structure. The effects of the reduced interlayer exchange coupling R_2, crystal field and the thickness of the unit cell on a and b ferromagnetic superlattices are given. The transition temperatures as a function of exchange interaction constants and crystal field are calculated. The obtained values are comparable to those given by the other theoretical results. The coercive field and the remnant magnetization have no influence when increasing the reduced exchange interaction R_2. The coercive field decreases with increasing the reduced crystal field and increases with increasing the size of the system.

References

[1] Dürr W, Taborelli M, Paul O, Germar R, Gudat W, Pescia D and Landolt M 1989 *Phys. Rev. Lett.* **62** 206
[2] Huang F, Mankey G J, Kief M T and Willis R F 1993 *J. Appl. Phys.* **73** 6760
[3] Baberschke K 1996 *Appl. Phys. A* **62** 417
[4] Wilhelm F, Bovensiepen U, Scherz A, Poulopoulos P, Ney A, Wende H, Ceballos G and Baberschke K 2000 *J. Magn. Magn. Mater.* **222** 163
[5] Verdier P, Ledue D and Patte R 2004 *J. Magn. Magn. Mater.* **271** 355
[6] Du A, Ma Y and Wu Z H 2006 *J. Magn. Magn. Mater.* **305** 233
[7] Tamion A, Ott F, Berche P E, Talbot E, Bordel C and Blavette D 2008 *J. Magn. Magn. Mater.* **320** 2650
[8] Özüm S, Yalçın O, Erdem R, Bayrakdar H and Eker H N 2015 *J. Magn. Magn. Mater.* **373** 217
[9] Wang J T, Zhou L, Wang D S and Kawazoe Y 2000 *Phys. Rev. B* **62** 3354
[10] Diaz-Ortiz A, Aguilera-Granja F and Moran-Lopez J L 1994 *Solid State Commun.* **914** 35
[11] Ou J T, Wang F and Lin D L 1997 *Phys. Rev. E* **56** 2805
[12] Saber M, Ainame A, Dujardin F and Stebe B 1999 *Phys. Rev. B* **59** 6908
[13] Kaneyoshi T and Shin S 2000 *Phys. State Solidi B* **218** 537
[14] Kaneyoshi T and Jaščur M 1994 *Physica A* **203** 316
[15] Kaneyoshi T and Jaščur M 1993 *J. Magn. Magn. Mater.* **118** 17
[16] Jaščur M and Kaneyoshi T 1995 *J. Magn. Magn. Mater.* **140–144** 488
[17] Honda S and Nawate M 1994 *J. Magn. Magn. Mater.* **136** 163
[18] Masrour R, Hamedoun M and Benyoussef A 2012 *Appl. Surf. Sci.* **258** 1902
[19] Masrour R, Bahmad L, Hamedoun M, Benyoussef A and Hlil E K 2014 *Phys. Lett. A* **378** 276
[20] Yüksel Y 2013 *Phys. Lett. A* **377** 2494
[21] Masrour R, Bahmad L and Benyoussef A 2013 *Chin. Phys. B* **22** 057504
[22] Bakrim H, Bouslykhane K, Hamedoun M, Hourmatallah A and Benzakour N 2004 *Surf. Sci.* **569** 219
[23] Zhang Q and Wei GZ 2002 *J. Magn. Magn. Mater.* **253** 96
[24] YükselY and AkıncıÜ 2015 *Physica B* **462** 54
[25] Bakrim H, Hamedoun M and Hourmatallah A 2003 *J. Magn. Magn. Mater.* **261** 415
[26] Masrour R, Jabar A, Benyoussef A, Hamedoun M and Bahmad L 2015 *Physica B* **472** 19
[27] Yuksel Y, Aydıner E and Polat H 2011 *J. Magn. Magn. Mater.* **323** 3168
[28] Ilkovic V 1998 *Thin Solid Films* **312** 280
[29] Tucker J W, Sarmento E F and Cressoni J C 1995 *J. Magn. Magn. Mater.* **147** 24
[30] Peng D L, Sumiyama K, Yamamuro S, Hihara T and Konno T J 1999 *Phys. Stat. Sol. (a)* **172** 209
[31] Santoro R P and Newnham R E 1967 *Acta Crystallogr.* **22** 344
[32] Szabó G and Kádár G 1998 *Phys. Rev. B* **58** 5584
[33] Cheng S F, Mansour A N, Teter J P, Hathaway K D and Kabacoff L T 1993 *Phys. Rev. B* **47** 206
[34] Cebollada A, Martnez J L, Gallego J M, de Miguel J J, Miranda R, Ferrer S, Batallán F, Fillion G and Rebouillat J P 1989 *Phys. Rev. B* **39** 9726
[35] Xiao G and Chien C L 1987 *J. Appl. Phys.* **61** 4061
[36] Sill L R, Brodsky M D, Bowen S and Hamaker H C 1985 *J. Appl. Phys.* **57** 3663
[37] Fu C L and Freeman A J 1987 *Phys. Rev. B* **35** 925
[38] Freemann A J, Xu J H and Jarlborg T 1983 *J. Magn. Magn. Mater.* **31** 909
[39] Yu A C C, Mizuno M, Sasaki Y and Kondo H 2002 *Appl. Phys. Lett.* **81** 3768
[40] Keskin M, Sarh N and Deviren B 2011 *Solid State Commun.* **151** 1025
[41] Marcano N, Gómez S J C, Espeso J I, De T J M, Algarabel P A, Paulsen C and Iglesias J R 2007 *Phys. Rev. Lett.* **98** 166406
[42] Cerisier M, Attenborough K, Celis J P and Van Haesendonck C 2000 *Appl. Surf. Sci.* **166** 154
[43] Tang X T, Wang G and Shima M 2006 *J. Appl. Phys.* **99** 123910